Structure-Governed Growth Phenomenon of a Trichosanthin Crystal

Bing Shi Li,[†] Geng Pei Li,[‡] Chen Wang,[†] Miao Wang,[§] Da Cheng Wang,[§] and Chunli Bai*,[†]

Center for Molecular Sciences, Institute of Chemistry, Chinese Academy of Sciences, Beijing 100080, China, Institute of Biophysics, Chinese Academy of Sciences, Beijing 100102, China, and Department of Chemistry, Peking University, Beijing 100871, China

Received April 9, 2002. In Final Form: July 11, 2002

We present the first results of in situ atomic force microscope observation of the growth phenomena of trichosanthin (TCS) crystals. It is observed that the three-dimensional (3D) nucleation provides a dominant growth pathway on the cystal surface, with two kinds of characteristic features, scalelike and domelike nuclei. The scalelike nuclei appear to assemble in the ⟨110⟩ direction, while domelike nuclei demonstrate a much faster growth in the ⟨1$\bar{1}$0⟩ direction. These particular growth phenomena are suggested to be determined by the unique molecular structures and interactions, according to the results of theoretical calculation. Along the ⟨110⟩ and ⟨1$\bar{1}$0⟩ directions, molecules are arranged in a way with their small domains binding the neighboring large domains, leading to strong hydrogen bonding between molecules. While along other directions, TCS molecules are associated with each other via weak van der Waals interactions. The diverse interactions along the different directions are responsible for the different binding behaviors of the molecules along different directions, which is further amplified as the selective assembling and asymmetry growth of (3D) nuclei along different directions.

1. Introduction

Crystal growth plays a crucial service role in the research of structural biology. Detailed structures of biological molecules can be obtained on high-quality protein crystals with the utilization of X-ray crystallography.[1,2] However, in contrast with the high demand for perfect crystals, much remains to be known about the underlying mechanisms of protein crystal growth.[3−5] Various techniques have been utilized in this field, such as quasi-elastic light scattering (QELS),[6−8] in situ Michelson interferometry,[9,10] dynamic light scattering (DLS),[11−13] dialysis kinetics,[14,15] freeze-etch electron microscopy,[16] and atomic force microscopy (AFM).[17,18] Among them, the biological applications of an atomic force microscope under liquid conditions allow direct observations of crystal growth in nearly physiological conditions. In addition to the surface structures, AFM could also be used to explore the dynamics parameters that govern macromolecule crystallization.[19] Slow growth rates and large molecular diameters make protein crystal an ideal system for in situ AFM investigation in the crystallization processes.[20] In the operation, a very sharp tip attached to a flexible cantilever scans over the surface of the crystal, which is immersed in the mother protein solution. Information of the growing surface can be recorded simultaneously in the process of crystal growth. Durbin and Carlson first used AFM to monitor the growth of the single crystal of lysozyme.[21] They revealed a mechanism, which is principally consistent with the classical model developed by Burton, Cabrera, and Frank.[22] With AFM's capability to discern the molecular-packing arrangements on the surface of crystal, investigation on macromolecular crystal growth can also be extended to molecular scale.[23−26] For instance, crystal growth is reported to proceed with an elementary step of bimolecules on the (110) face of the lysozyme; growth of canavalin is observed to advance on

* To whom correspondence should be addressed. Tel: 86-10-62568158. Fax: 86-10-62557908. E-mail: clbai@infoc3.icas.ac.cn.
[†] Institute of Chemistry, Chinese Academy of Sciences.
[‡] Department of Chemistry, Peking University.
[§] Institute of Biophysics, Chinese Academy of Sciences.

(1) McPherson, A. *Int. Union Crystallogr.* **1998**, *6*, 5.
(2) McPherson, A. *Eur. J. Biochem.* **1990**, *189*, 1.
(3) Koszelak, S.; Day, J.; Leja, C.; Cudney, R.; McPherson, A. *Biophys. J.* **1995**, *69*, 13.
(4) Matthews, B. W. *J. Mol. Biol.* **1968**, *33*, 491.
(5) Delucas, L. J.; Suddath, F. L.; Snyder, R.; Naumann, R.; Broom, M. B.; Pusey, M. L.; Yost, V.; Herren, B. *J. Cryst. Growth* **1986**, *76*, 681.
(6) Malkin, A. J.; McPherson, A. *J. Cryst. Growth* **1993**, *128*, 1232.
(7) Malkin, A. J.; McPherson, A. *Acta Crystallogr.* **1993**, *D50*, 385.
(8) Malkin, A. J.; McPherson, A. *J. Cryst. Growth* **1993**, *126*, 555.
(9) Kuznetsov, Y. G.; Malkin, A. J.; Greenwood, A.; McPherson, A. *J. Cryst. Growth* **1996**, *166*, 913.
(10) Kuznetsov, Y. G.; Malkin, A. J.; Greenwood, A.; McPherson, A. *J. Struct. Biol.* **1995**, *114*, 184.
(11) Sazaki, G.; Oshima, H.; Harano, Y.; Hirokawa, N. *J. Cryst. Growth* **1993**, *130*, 357.
(12) Thibault, F.; Langowski, J.; Leberman, R. *J. Cryst. Growth* **1992**, *122*, 50.
(13) Skouri, M.; Munch, J. P.; Lober, B. *J. Cryst. Growth* **1992**, *122*, 14.
(14) Wilson, L. J.; Adcock, L. D.; Pusey, M. L. *Biophys. J.* **1996**, *71*, 2123.
(15) Wilson, L. J.; Adcock, L. D.; Pusey, M. L. *J. Phys. D.*: *Appl. Phys.* **1993**, *26*, B113.
(16) Durbin, S. D.; Feher, G. *J. Mol. Biol.* **1990**, *212*, 763.
(17) Hillner, P. E.; Manne, S.; Hansma, P. K., Gratz, A. J. *Faraday Discuss.* **1993**, *95*, 191.
(18) Durbin, S. D.; Warren, E. C.; Saros, M. T. *J. Phys. D*: *Appl. Phys.* **1993**, *26*, B128.
(19) Drake, B.; Prater, C. B.; Weisenhorn, A. L.; Gould, S. C.; Albecht, T. R.; Quate, C. F.; Cannell, D. S.; Hansma, H. G.; Hansma, P. K. *Science* **1989**, *243*, 1586.
(20) Kuznetsov, Y. G.; Malkin, A. J.; Glantz, W.; McPherson, A. *J. Cryst. Growth* **1996**, *168*, 63.
(21) Durbin, S. D.; Warren, E. C. *J. Cryst. Growth* **1992**, *122*, 71.
(22) Burton, W. K.; Cabrera, N.; Frank, F. C.; *Philos. Trans. R. Soc. London* **1951,** *A243*, 299.
(23) Kuznetsov, Y. G.; Malkin, A. J.; Land, T. A.; De Yoreo, J. J.; Barba, A. P. Konnert, J. H.; McPherson, A. *Biophys. J.* **1997**, *72*, 2367.
(24) Li, H.; Nadarajah, A.; Pusey, M. L. *Acta Crystallogr.* **1999**, *D55*, 1036.
(25) Li, H.; Peozzo, M. A.; Connert, J. H.; Nadarajah, A.; Pusey, M. L. *Acta Crystallogr.* **1999**, *D55*, 1023.
(26) Konnert, J. H.; Antonio, P. D.; Ward, K. B. *Acta Crystallogr.* **1994**, *D50*, 603.

10.1021/la0258190 CCC: $22.00
Published on Web 08/10/2002

single trimer steps on (100) plane of canavalin. In situ AFM has been applied to the study of the growth of protein and virus crystals (canavalin, thaumatin, catalase, apoferritin, lysozyme, and STMV).[20,26−28] Macromolecules in general adopt similar growth mechanisms with that of conventional molecules, namely, by spiral dislocations, two-dimensional (2D) and three-dimensional (3D) nucleation. In addition, they do have other unique growth features, which were related with the different magnitudes of the underlying kinetics and the thermodynamics parameters that govern the growth process.[29−36] Up until now, in situ AFM has only been applied to limited types of macromolecular crystals, due to the practical problem in the experiment.

This work is focused on in situ AFM studys of the crystal growth of TCS in nearly native solution environment and exploiting the interesting growth phenomena from the observed molecular structures. The results revealed two types of characteristic features for the 3D nucleation growth process. The scalelike nuclei appear to assemble in a ⟨110⟩ direction, while domelike nuclei demonstrate a much faster growth in the ⟨1$\bar{1}$0⟩ direction. Such unique growth phenomena are suggested to be governed by the unique molecular structures, which further lead to diversity interactions along different directions.

2. Experimental Section

TCS is a type I ribosome-inactivating (RIP_3) protein extracted from *trichosanches kirilowii maxim* (M_r = 26 000 Da).[37] Three different types of crystals (monoclinic $P2_1$, C_2, and orthorhombic $P2_12_12_1$) have been grown with various precipitants within the pH range from 5.4 to 8.7, using vapor diffusion in a hanging-drop method. The crystal structure has already been determined at various resolutions.[38,39] The unit cell of the orthorhombic TCS (a = 3.8 nm, b = 7.7 nm, c = 7.9 nm, space group $P2_12_12_1$) consists of two TCS layers paralleling to (001), each layer related by a 2_1 screw axis paralleling the c axis or b axis. The orthorhombic single crystals of TCS were obtained by vapor diffusion from a solution containing 30 mg/mL TCS, buffered with 0.5 M Na_3Cit (pH = 5.4), using 3 M KCl as the precipitant at room temperature (295 ± 0.1 K). TCS crystals can grow up to a maximum dimension of about 1 mm within a week, and those around 0.5 mm (the third day of culturing) were selected for AFM experiments.

Crystals suitable for AFM observation were gently transferred to a stainless steel disk, which was magnetically secured to the AFM scanner base. About 40 μL of mother protein solution was added to the fluid cell with an O-ring forming a seal on the stainless disk to prevent evaporation so that stable images might be obtained within several hours. Images were collected in a contact mode with a Nanoscope III atomic force microscope (Digital Instruments, Santa Barbara, CA) using a cantilever with a nominal force constant 0.06 N/m. Data of height mode and deflection mode were both recorded. During the course of the experiments, the force applied to the surface of the crystal can be adjusted to 0.1−0.2 nN by moderating the setpoint value.

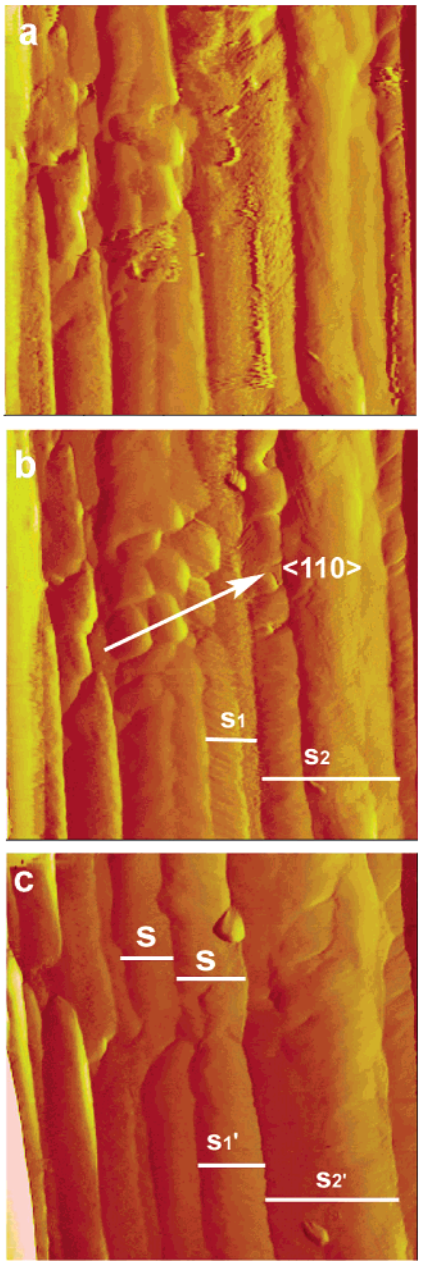

Figure 1. (a−c) Sequence of 13 × 13 μm^2 in situ AFM images showing scalelike nucleation, assembling, and coalescence on the (001) plane of TCS crystals. Steps in panel b labeled with lines S_1 and S_2 converge into wider steps labeled with S_1' and S_2', respectively. Steps labeled with S in panel c are generated by the coalescence of scalelike nuclei. Images from (a) to (c) were recorded at 0, 15, and 35 min, respectively.

3. Results and Discussion

3.1. 3D Nucleation Growth Phenomenon of TCS Crystal. Three-dimensional nucleation is found to be a dominant pathway of the growth of the (001) plane of TCS crystals, namely, by scalelike and domelike nucleation. The scalelike nuclei appear either on the terraces or on the surfaces of the steps, as shown in panels a and b of Figure 1. It is observed that the newly formed nuclei often appear adjacent to the already existent ones along the ⟨110⟩ direction, as indicated in Figure 1b. The nuclei continue to grow and coalesce with each other to form parallel steps. As illustrated in Figure 1c, newly generated

(27) Mcpherson, A.; Malkin, A. J.; Kuznestsov, Y. G.; Plomp, M. *Acta Crystallogr.* **2001**, *D55*, 1053.
(28) Land, T. A.; De Yoreo, J. J. *J. Cryst. Growth* **2000**, *208*, 623.
(29) Land, T. A.; Malkin, A. J.; Kuzenetsov, Y. G.; McPherson, A.; De Yoreo, J. J. *Phys. Rev. Lett.* **1995**, ***75***, 2774.
(30) Land, T. A.; Malkin, A. J.; Kuzenetsov, Y. G.; McPherson, A. De Yoreo, J. J. *J. Cryst. Growth* **1996**, *166*, 893.
(31) De Yoreo, J. J.; Land, T. A.; Lee, J. D. *Phys. Rev. Lett.* **1997**, *78*, 4462.
(32) Feher, G. *J. Cryst. Growth* **1986**, *76*, 545.
(33) Feigelson, R. S. *J. Cryst. Growth* **1998**, *90*, 1.
(34) McPherson, A. *Structure* **1995**, *3*, 759.
(35) Malkin, A. J.; Kuznetsov, Y. G.; Land, T. A.; De Yoreo, J. J.; McPherson, A. *Nat. Struct. Biol.* **1995**, *2*, 956.
(36) Land, T. A.; De Yoreo, J. J.; Lee, J. D. *Surf. Sci.* **1997**, *384*, 136.
(37) Wang, J. H.; Wang, Y. P.; Tian, G. Y. *Chin. Sci. Bull.* **1984**, *12*, 943.
(38) Ma, X. Q.; Wang, Y. P.; Wang, J. H. *Sci. Sin. Ser.* **1987**, *B7*, 705.
(39) Pan, K.; Zhang, Y.; Lin, Y.; Wu, Z.; Zheng, A.; Cheng, Y.; Dong, Y.; Ma, X.; Wang, Y.; Wu, S.; Zhang, M.; Chen, S.; Xia, Z.; Tian, G.; Ni, C.; Fan, Z.; Ma, Y.; Sun, X. *Sci. Sin. Ser.* **1986**, *B1*, 26.

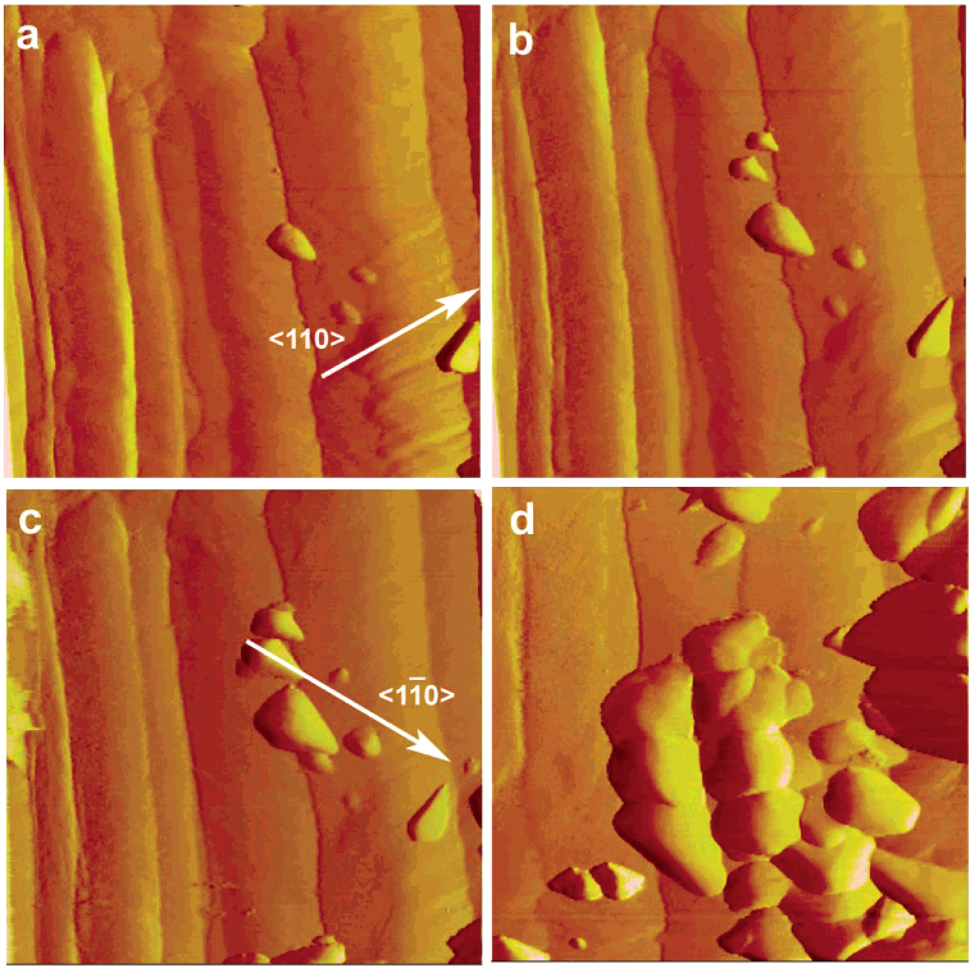

Figure 2. (a−d) Sequence of 13 × 13 μm^2 in situ AFM images showing the domelike nucleation, growth, and coalescence. Images from (a) to (d) were recorded at 0, 10, 20, and 50 min.

steps labeled with S can be easily observed. Dome-shaped 3D nuclei are also observed on the growing surface of the crystal, as shown in Figure 2. Of particular interest, the shape of the nuclei is asymmetric due to the considerably fast growth in the $\langle 1\bar{1}0\rangle$ direction. The nuclei finally merge with each other along the $\langle 100\rangle$ direction to form convex surfaces.

Three-dimensional nucleation for macromolecular crystal growth has been reported in three systems, STMV, thaumatin, and canavalin.[20,35] It was the dominant source of growth as in the case of STMV and at sufficiently high supersaturation for thaumatin. For canavalin, 3D nucleation has been shown to be a growth pathway that competes with the 2D nucleation process. The 3D nuclei of these crystals all possess flat surfaces and stacks can be further formed with a layer by layer addition of 3D nuclei in all the above systems. In sharp contrast to the 3D nucleation of the above systems, both scalelike and domelike nuclei of TCS crystals provide only convex surfaces. The newly formed nuclei are therefore observed to adsorb adjacent to the already existent ones, instead of adsorbing directly on top of existent nuclei, excluding the formation of stacks. It is especially rare that the scalelike nuclei tend to assemble in a certain direction instead of random adsorption, revealing a somewhat different growth phenomenon from the 3D nucleation of the reported macromolecular crystals.

It is also worth mentioning here that steps were also observed on the growing surface of TCS crystals in conjunction with scalelike and domelike nucleation, as shown in Figure 1 and Figure 2. They are more like step bunches, considering their irregular shapes and appreciable magnitude in height. The steps can be formed by coalescence of the scalelike nuclei as mentioned above or by merging of multiple adjacent steps. As indicated in Figure 1b and Figure 1c, two nearly parallel groups of adjacent narrow steps labeled S_1 converge to form a wider step labeled S_1' and a similar case can be found with S_2 and S_2'. The extension of the steps along $\langle 001\rangle$ is usually found to be accompanied with the merging of the adsorbates, as shown in Figure 2a. The extruding surfaces and the significant variance in step height make the growing surface rather rough and hamper the observation of elementary steps. For the same reason, larger scanning images are difficult to obtain. A complete evolution of the steps needs to be clarified with more evidence.

3.2. Interpretation of the Growth Phenomenon from Crystal Structures. The assembly of the scalelike nuclei is rarely observed for other reported crystals. The growth phenomenon is suggested to be inherently determined by the unique chemical structures of the molecules and their arrangement in the crystal. As shown in the left ribbon diagram in Figure 3,[37−39] there are two domains in the structure of the TCS molecule: the N-terminal one is larger, containing about 160 residues, while the smaller C-terminal domain has about 60 residues and the last few residues just lie between the two domains. The polar residues, which may attribute to the strong interactions between molecules, are mainly concentrated in the contact interfaces of the two domains and the small domains. The model of the orthorhombic TCS crystal structure (the right diagram in Figure 3) shows that each TCS molecule in

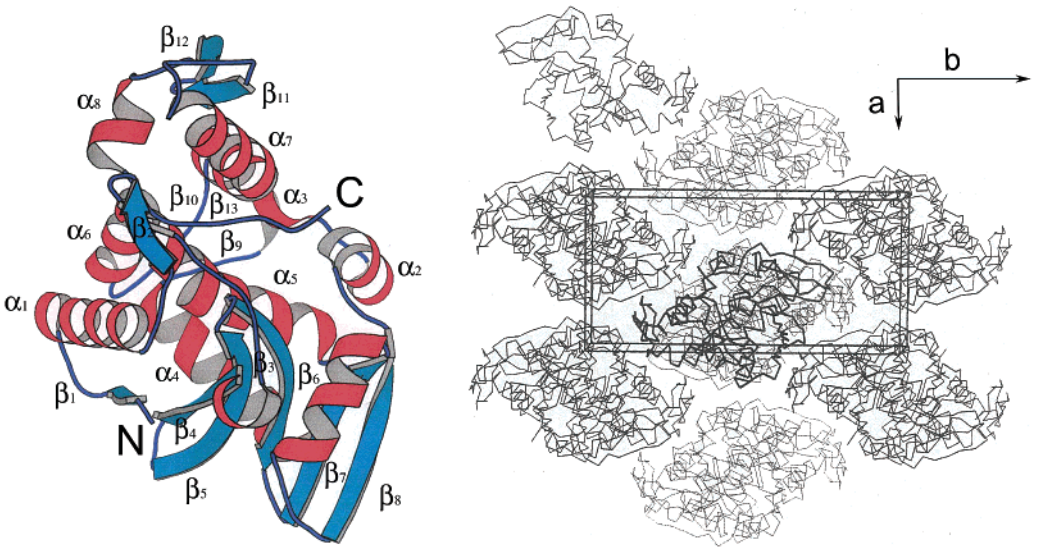

Figure 3. (left) Ribbon diagram of the TCS molecule. (right) Arrangement of TCS molecules in the $P2_12_12_1$ lattice viewed from crystallography C. The central molecule, in heavy line, is the reference molecule. The TCS molecules occur in pseudohexagonal stacked ABABAB in a close-packed fashion. The solvent channels run parallel to the crystallographic ab plane. (Both models were prepared using MOLSCRIPT (Kraulis, 1991).)

the orthorhombic $P2_12_12_1$ crystal lattice interacts with eight symmetry-related molecules, with six molecules associated strongly in the (001) plane to form distinct layers and the remaining two are at the above and the below plane with a weak molecular interaction, respectively. The molecules along ⟨110⟩ and ⟨1$\bar{1}$0⟩ are assembled with their small domains binding the neighboring ones' large domains. Multiple H-bonds are formed along these directions, and interactions between molecules are further enhanced with a hydrophobic effect summed by individual hydrophobic residues, such as the interaction between helix $\alpha_{2,3}$ and β-sheets of $\beta_{9,10}$. Along other directions, TCS molecules are arranged in a way with large−large or small−small domains binding each other. H-bonds can thus hardly form, and molecules interact with weak VDW. Especially, the molecular interaction along ⟨001⟩ direction is rather weak with an additional influence of water layers at half-unit cell intervals along *c* axis.

The different molecular interactions and the packing pathway of TCS molecules at different directions provide consistent theoretical evidences with the observed growth phenomena of TCS crystal. Selective assembling of 3D scale-like nuclei along ⟨110⟩ and faster growth of domelike 3D nuclei along ⟨1$\bar{1}$0⟩ could both be attributed to the higher strength of association of molecules along these directions. While the slowest growth rate along ⟨001⟩ can be considered in close relation with the weak molecular interaction along this direction. TCS molecules are jointed together with weak van der Waals interactions and not strong enough to bind molecules along this direction, which consequently results in slow growth.

4. Conclusion

A dominant 3D nucleation growth mechanism is adopted by TCS crystals observed by AFM, with two kinds of characteristic features, scalelike and domelike nuclei. Different from the reported 3D nucleation processes, the scalelike nuclei show a selective assembling in the ⟨110⟩ direction and the domelike nuclei demonstrate a much faster growth in the ⟨1$\bar{1}$0⟩ direction. The observed growth phenomena are attributed to the unique molecular structures, leading to diverse interactions along different directions.

Acknowledgment. This work was supported by National Science Foundation of China (No. 20025308, 20177025) and National Key Project on Basic Research (Grant G2000077501).

LA0258190